Inorg. Chem. **2007**, *46*, 2017–2027

Synthesis of a Family of Solids through the Building-Block Approach: A Case Study with Ag^+ Substitution in the Ternary Na–Ge–Se System

Amitava Choudhury, Sabine Strobel, Benjamin R. Martin, Angela L. Karst, and Peter K. Dorhout*

Department of Chemistry, Colorado State University, Fort Collins, Colorado 80523

Received June 13, 2006

A new family of Ag-substituted pseudoquaternary alkali-seleno-germanates has been synthesized by two solid-state routes: the conventional flux method and metathesis. This family includes a series of semiconductors with varying amounts of Ag^+ substituted for Na^+ in $Na_8Ge_4Se_{10}$ to form $Ag_xNa_{(8-x)}Ge_4Se_{10}$, [$x = 0.31$ (**I**), 0.67 (**II**), 0.77 (**III**), 0.87 (**IV**), 1.05 (**V**), 1.09 (**VI**)] and another phase with a different composition $Ag_xNa_{(6-x)}Ge_2Se_7$ ($x = 1.76$), **VII**, related to $Na_6Ge_2Se_7$. In **I**–**VI**, $Ge_4Se_{10}^{8-}$ constitutes a 6-membered chairlike unit with a Ge–Ge bond, while in **VII**, a corner-shared dimer of $GeSe_4$ tetrahedra ($Ge_2Se_7^{6-}$) acts as the building unit. The single-crystal structure analysis indicates that there is a phase transition from $P\bar{1}$ to $C2/c$, in changing from pure $Na_8Ge_4Se_{10}$ to $Ag_xNa_{(8-x)}Ge_4Se_{10}$ (**I**–**VI**), while there is no phase transition between pure $Na_6Ge_2Se_7$ and $Ag_xNa_{(6-x)}Ge_2Se_7$ ($x = 1.76$). The structures of **I**–**VI** may be described in terms of layers of cubic close-packed Se^{2-} anions. In between the Se layers, octahedral holes fully occupied by Na^+ and mixed Ag^+/Na^+ cations alternate with layers formed of octahedral holes fully occupied by Na^+ and Ge_2^{6+} cations. Two adjacent Ge_2^{6+} cations form a chairlike $Ge_4Se_{10}^{8-}$ anion in which Ge–Ge bonds are oriented almost parallel to the Se layers. In contrast, **VII** does not have close-packed anions. Corner-shared $GeSe_4$ tetrahedra ($Ge_2Se_7^{6-}$ dimer) and $AgSe_4$ tetrahedra form layers that are cross-linked by $Na/AgSe_4$ tetrahedra to form a 3-dimensional (3-D) structure. An optical property investigation indicates a red shift in the band gap of $Ag_xNa_{(8-x)}Ge_4Se_{10}$ ($x = 0.67$)(**II**) as compared to that of pure $Na_8Ge_4Se_{10}$. Raman data also indicate a red shift of the Ge–Se stretching mode in the Ag^+-substituted phase **II** ($x = 0.67$) compared to that of $Na_8Ge_4Se_{10}$.

Introduction

Ternary and quaternary compounds involving main group metal chalcogenide building blocks have received recent attention because of their rich structural chemistry[1,2] and useful physical and chemical properties for potential applications in nonlinear optics,[3] ferroelectrics,[4] and thermoelectric materials.[5] The ability of the main group metal chalcogenide-based anions to form various building units, which can participate in the construction of complex networks in combination with other metals in ternary or quaternary compounds, makes them more attractive. These building units in the chalco-germanate family of solids include, for example, isolated tetrahedra (GeQ_4^{4-}, Q = Se, S),[6] corner ($Ge_2Q_7^{6-}$) and edge-sharing ($Ge_2Q_6^{4-}$) tetrahedra,[7,8] ethane-like units ($Ge_2Q_6^{6-}$),[9] adamantane units ($Ge_4Q_{10}^{4-}$),[10] 5- and 6-membered ring units ($Ge_4Se_{10}^{8-}$),[11,9b] as well as networks of corner-sharing chains of tetrahedra

* To whom correspondence should be addressed. Fax: 970-491-1801. E-mail: pkd@lamar.colostate.edu.

(1) Krebs, B. *Angew. Chem., Int. Ed. Engl.* **1983**, *22*, 113.
(2) Sheldrick, W. S.; Wachhold, M. *Coord. Chem. Rev.* **1998**, *176*, 211.
(3) Liao, J. H.; Marking, G. A.; Hsu, K. F.; Matsushita, Y.; Ewbank, M. D.; Borwick, R.; Cunningham, P.; Rosker, M. J.; Kanatzidis, M. G. *J. Am. Chem. Soc.* **2003**, *125*, 9484.
(4) Tampier, M.; Johrendt, D. *J. Solid State Chem.* **2001**, *158*, 343.
(5) (a) Sales, B. C.; Mandrus, D.; Williams, R. K. *Science* **1996**, *272*, 1325. (b) DiSalvo, F. J. *Science* **1999**, *285*, 703. (c) Chung, D.-Y.; Hogan, T.; Brazis, P.; Rocci-Lane, M.; Kannewurf, C.; Bastea, M.; Uher, C.; Kanatzidis, M. G. *Science* **2000**, *287*, 1024. (d) Venkatasubramanian, R.; Slivola, E.; Colpitts, T.; O'Quinn, B. *Nature* **2001**, *413*, 597. (e) Hsu, K. F.; Loo, S.; Guo, F.; Chen, W.; Dyck, J. S.; Uher, C.; Hogan, T.; Polychroniadis, E. K.; Kanatzidis, M. G. *Science* **2004**, *303*, 818. (d) McGuire, M. A.; Reynolds, T. K.; DiSalvo, F. J. *Chem. Mater.* **2005**, *17*, 2875. (e) McGuire, M. A.; Scheidemantel, T. J.; Badding, J. V.; DiSalvo, F. J. *Chem. Mater.* **2005**, *17*, 6186.
(6) Klepp, K. O. *Z. Naturforsch.* **1985**, *40*, 878.
(7) (a) Jumas, J. C.; Olivier-Fourcade, J.; Vermot-Gaud-Daniel, F.; Ribes, M.; Philippot, E.;Maurin, M. *Rev. Chim. Miner.* **1974**, *11*, 13. (b) Eisenmann, B.; Hansa, J.; Schaefer, H. *Rev. Chim. Miner.* **1986**, *23*, 8.
(8) (a) Eisenmann, B.; Hansa, J. *Z. Kristallogr.* **1993**, *203*, 301. (b) Klepp, K. O.; Fabian, F. *Z. Kristallogr.* **1997**, *212*, 302. (c) Preishuber-Pfluegl, H.; Klepp, K. O. *Z. Kristallogr.* **2003**, *218*, 387. (d) Almsick, T. V.; Sheldrick, W. S. *Z. Anorg. Allg. Chem.* **2005**, *631*, 1746.

10.1021/ic061064z CCC: $37.00
Published on Web 02/16/2007

(GeQ_3^{2-})[11] or lamellar $(Ge_2Q_5^{2-})$[12] solids. Very often, these finite anionic building units are excellent tools for designing complex solids. It has already been demonstrated by Yaghi, for example, that one can construct open-framework materials using the admantane unit ($Ge_4S_{10}^{4-}$) in solution.[13] In solids, it has been observed that a particular building unit, which is stabilized by alkali metal ions in ternary compounds,[6−11] also exists in quaternary compounds along with a second metal ion: for example, isolated tetrahedra in $ALnGeQ_4$ (A = alkali metal, Ln = lanthanides),[14] ethane-like dimers in $Na_8M(Ge_2S_6)_2$ (M = Sn, Pb, Eu) and $Na_9Ln(Ge_2Se_6)_2$,[15] and edge-shared dimers in $K_2Au_2Ge_2S_6$, $K_2PbGe_2S_6$, and $A_2Eu(Ge_2Se_6)_2$ (A = K, Rb, Cs).[16] However, there have been few successful efforts to design solids by purposefully incorporating a "building-block" in the solid-state synthetic technique forming new structures. The ability to utilize the distinct types of "building-blocks" of ternary compounds in different quaternary compounds by partial substitution of alkali metals through a metathesis reaction with other metal salts using solid-state synthesis techniques is especially important because it represents an approach to the rational design of solids with the potential of fine-tuning their properties. The simplest approach in this regard would be the controlled introduction of +1 ionic metals, such as the coinage metals (Cu, Ag, Au), in place of alkali metals in ternary alkali chalcogermanates. The substitution of less-electropositive and somewhat larger cations like silver for a sodium cation might lead to considerable changes in the crystal structure and electronic properties because of the greater covalent nature of the Ag−Se bonds compared to a predominantly electrostatic interaction in the A−Se bonds (A = alkali metal). To test this hypothesis, we attempted to substitute Ag^+ cations in a structure of $Na_8Ge_4Se_{10}$, while maintaining the integrity of the six-membered chairlike unit ($Ge_4Se_{10}^{8-}$) and also tune its band gap. In this article, we describe the synthesis, structural characterization, and optical properties of a series of compounds of the composition $Ag_xNa_{8-x}Ge_4Se_{10}$ (x = 0.31, 0.67, 0.77, 0.87, 1.05, 1.09), where the chairlike building unit remains intact but the structure undergoes a phase transition from the phase of pure $Na_8Ge_4Se_{10}$. We also report the structure of a second Ag-substituted compound, $Ag_xNa_{6-x}Ge_2Se_7$, where corner-shared dimers of $GeSe_4$ tetrahedra ($Ge_2Se_7^{6-}$) found in ternary $Na_6Ge_2Se_7$ remain intact and there is no accompanying phase transition.

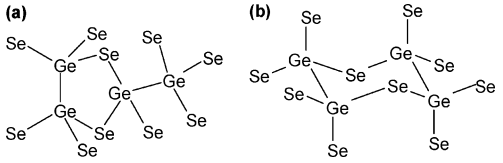

Figure 1. Schematic representations of the five- and six-membered ring $Ge_4Se_{10}^{8-}$ units found in the two polymorphs of $Na_8Ge_4Se_{10}$: (a) $Na_8Ge_4Se_{10}$-5M and (b) $Na_8Ge_4Se_{10}$-6M.

Experimental Section

Synthesis. The compounds were prepared by the reaction of elemental Ge, Se, and Ag with the binary Na_2Se_2 or by solid-state metathesis reactions using preformed salts such as $Na_8Ge_4Se_{10}$. Ge (99.999%, Cerac), Se (99.999%, Johnson-Mathey), and Ag (99.99%, −325 mesh, Cerac) were used as received, and Na_2Se_2 was prepared from the stoichiometric combination of the elements in liquid ammonia as described previously.[17] Reactants were loaded into fused silica ampules inside an N_2-filled glove box. The ampules were flame-sealed under vacuum and placed in a temperature-controlled furnace. The furnace was ramped to 725 °C at a rate of 35 °C/h, and the temperature was held constant at 725 °C for 150 h. The furnace was then slowly cooled to ambient temperature at a rate of 5 °C/h. After the reaction products cooled, the ampules were opened in an inert atmosphere glove box, and the solid product was soaked in dry *N*,*N*-dimethylformamide (DMF) and sonicated for 1 min to dissolve and wash away any remaining flux and loosen the product crystals. The semiquantitative EDAX analysis on individual crystals of each reaction product confirms the presence of Ag, Ge, Se, and Na. The color of the crystals varied from orange to red as the concentration of the Ag^+ ion increased. The compounds were modestly stable in air; however, they decomposed gradually under longer exposure to air and light.

In the $Ag_xNa_{(8-x)}Ge_4Se_{10}$ (**I**−**VI**) series of compounds, $Ag_{0.87}Na_{7.13}Ge_4Se_{10}$ (**IV**) was first isolated accidentally while attempting to synthesize the pseudoquinary rare-earth chalcogenide, $Ag_xNa_{(1-x)}SmGeSe_4$. Subsequently, we have found another composition, $Ag_{0.31}Na_{7.69}Ge_4Se_{10}$ (**I**), without using Sm in the reaction mixture. $Ag_{0.87}Na_{7.13}Ge_4Se_{10}$ (**IV**) was synthesized by combining 15.4 mg of Sm (0.1 mmol), 43.2 mg of Ag (0.4 mmol), 30 mg of Ge (0.4 mmol), 47.4 mg of Se (0.6 mmol), and 61.2 mg of Na_2Se_2 (0.3 mmol). The final ratio of the starting reactants was Sm/4 Ag/ 6 Na/4 Ge/12 Se. The product contained red plates and irregularly shaped orange crystals. The red plates were identified as the known compound $Na_9Sm(Ge_2Se_6)_2$ by matching of the unit cells collected on a single-crystal diffractometer.[15b] The orange crystals that did not contain any Sm (based on EDAX analysis) turned out to be the new compound **IV**. $Ag_{0.31}Na_{7.69}Ge_4Se_{10}$, **I**, on the other hand was synthesized in the absence of Sm, while the Ag and Na ratio was varied; 36.8 mg of Ag (0.34 mmol), 33.1 mg of Ge (0.45 mmol), 35.9 mg of Se (0.45 mmol), and 92.8 mg of Na_2Se_2 (0.45

(9) (a) Eisenmann, B.; Kieselbach, E.; Schaefer, H.; Schrod, H. *Z. Anorg. Allg. Chem.* **1984**, *516*, 49. (b) Eisenmann, B.; Hansa, J.; Schaefer, H. *Mater. Res. Bull.* **1985**, *20*, 1339. (c) Schlirf, J.; Deiseroth, H.-J. *Z. Kristallogr.* **2001**, *216*, 27.
(10) (a) Philippot, E.; Ribes, M.; Lindqvist, O. *Rev. Chim. Miner.* **1971**, *8*, 477. (b) Klepp, K. O.; Fabian, F. *Z. Naturforsch.* **1999**, *b54*, 1499. (c) Klepp, O. K; Zeitlinger, M. *Z. Kristallogr.* **2000**, *215*, 7.
(11) Eisenmann, B.; Hansa, J.; Schaefer, H. *Z. Naturforsch.* **1985**, *b40*, 450.
(12) Eisenmann, B.; Hansa, J.; Schaefer, H. *Rev. Chim. Miner.* **1984**, *21*, 817.
(13) Yaghi, O. M.; Sun, Z.; Richardson, D. A.; Groy, T. L. *J. Am. Chem. Soc.* **1994**, *116*, 807.
(14) (a) Wu, P.; Ibers, J. A. *J. Solid State Chem.* **1993**, *107*, 347. (b) Bucher, C. K.; Hwu, S. -J. *Inorg. Chem.* **1994**, *33*, 5831. (c) Evenson, C. R.; Dorhout, P. K. *Inorg. Chem.* **2001**, *40*, 2409. (d) Martin. B. R.; Dorhout, P. K. *Inorg. Chem.* **2004**, *43*, 385. (e) Chan, B. C.; Dorhout, P. K. *Z. Kristallogr.: New Cryst. Struct.* **2005**, *220*, 7.
(15) (a) Marking, G. A.; Kanatzidis, M. G. *J. Alloys Compd.* **1997**, *259*, 122. (b) Martin, B. R.; Polyakova, L. A.; Dorhout, P. K. *J. Alloys Compd.* **2005**, *408*−*412*, 490. (c) Martin, B. R.; Knaust, J. M.; Dorhout, P. K. *Z. Kristallogr.: New Cryst. Struct.* **2005**, *220*, 294. (d) Knaust, J. M.; Polyakova, L. A.; Dorhout, P. K. *Z. Kristallogr.: New Cryst. Struct.* **2005**, *220*, 295.
(16) (a) Löken, S.; Tremel, W. *Z. Anorg. Allg. Chem.* **1998**, *624*, 1588. (b) Palchik, O.; Marking, G. M.; Kanatzidis, M. G. *Inorg. Chem.* **2005**, *44*, 4151. (c) Polyakova, L. A.; Dorhout, P. K. Manuscript in preparation.
(17) (a) Schewe-Miller, I. Metallreiche hauptgruppenmetall-Chalkogenverbindungen: Synthese, Strukturen and Eigenschaften. Ph.D. Thesis, Max-Planck-Institut fur Festkorperforschung, Stuttgart, Germany, 1990. (b) Liao, J.-H.; Kanatzidis, M. G. *Inorg. Chem.* **1992**, *31*, 431.

Table 1. Ratio and the Absolute Quantities of the Starting Reactants and the Composition of the Final Product

	reactants				Ag/Na	final composition
II	2Ag (107.8)[a]	4Ge (145.2)	4Se (157.9)	$3Na_2Se_2$ (305.8)	2:6	$Ag_{0.67}Na_{7.33}Ge_4Se_{10}$
V	6Ag (145.7)	4Ge (65.4)	8Se (142.2)	Na_2Se_2 (45.9)	6:2	$Ag_{1.04}Na_{6.95}Ge_4Se_{10}$
VI	4Ag (108)	4Ge (72.7)	6Se (118.6)	$2Na_2Se_2$ (102.1)	4:4	$Ag_{1.09}Na_{6.91}Ge_4Se_{10}$
VII	Ag (53.9)	4Ge (145.2)	3Se (118.4)	$3.5Na_2Se_2$ (356.8)	1:7	$Ag_{1.76}Na_{4.24}Ge_2Se_7$

[a] The numbers in the parentheses indicate absolute quantities of the reactants in milligrams.

Table 2. Crystal Data and Structure Refinement for the Compounds **I**−**VII**

	I	**II**	**III**	**IV**
chemical formula	$Ag_{0.31}Na_{7.69}Ge_4Se_{10}$	$Ag_{0.67}Na_{7.33}Ge_4Se_{10}$	$Ag_{0.77}Na_{7.23}Ge_4Se_{10}$	$Ag_{0.87}Na_{7.13}Ge_4Se_{10}$
fw	1290.40	1320.96	1329.24	1337.73
space group	*C2/c* (No. 15)	*C2/c* (No. 15)	*C2/c* (No. 15)	*C2/c* (No. 15)
temp (K)	298	298	298	298
wavelength (Å)	0.71073	0.71073	0.71073	0.71073
a (Å)	8.101(2)	8.104(2)	8.104(2)	8.1030(9)
b (Å)	20.147(6)	20.163(3)	20.156(5)	20.155(3)
c (Å)	14.063(4)	13.998(2)	13.985(4)	13.9665(9)
α (deg)	90.0	90.0	90.0	90.0
β (deg)	106.182(5)	105.861(3)	105.757(4)	105.699(2)
γ (deg)	90.0	90.0	90.0	90.0
vol (Å^3)	2204.2(1)	2200.3(6)	2198.5(5)	2195.9(5)
Z	4	4	4	4
ρ_{calcd} (Mg m^{-3})	3.888	3.988	4.016	4.046
μ (mm^{-1})	22.321	22.664	22.766	22.877
R [$F^2 > 2\sigma(F^2)$][a]	0.0507	0.0332	0.0551	0.0455
wR (F^2) (all data)[b]	0.1532	0.0860	0.1424	0.0917

	V	**VI**	**VII**
chemical formula	$Ag_{1.04}Na_{6.95}Ge_4Se_{10}$	$Ag_{1.09}Na_{6.91}Ge_4Se_{10}$	$Ag_{1.76}Na_{4.24}Ge_2Se_7$
fw	1352.58	1355.97	985.02
space group	*C2/c* (No. 15)	*C2/c* (No. 15)	*C2/c* (No. 15)
temp (K)	298	298	298
wavelength (Å)	0.71073	0.71073	0.71073
a (Å)	8.098(4)	8.1013(7)	9.7234(18)
b (Å)	20.131(9)	20.1342(8)	10.547(2)
c (Å)	13.922(6)	13.9213(3)	15.236(3)
α (deg)	90.0	90.0	90
β (deg)	105.547(9)	105.541(2)	102.985(3)
γ (deg)	90.0	90.0	90
vol (Å^3)	2186.4(7)	2187.7(3)	1522.5(5)
Z	4	4	4
ρ_{calcd} (Mg m^{-3})	4.109	4.117	4.297
μ (mm^{-1})	23.125	23.145	22.959
R [$F^2 > 2\sigma(F^2)$][a]	0.0476	0.0440	0.0429
wR (F^2) (all data)[b]	0.0945	0.0935	0.1131

[a] $R1 = \sum||F_o| - |F_c||/\sum|F_o|$. [b] $wR2 = \{\sum[w(F_0^2 - F_c^2)^2]/\sum[w(F_0^2)^2]\}^{1/2}$, $w = 1/[\sigma^2(F_o)^2 + (aP)^2 + bP]$ where $P = [F_o^2 + 2F_c^2]/3$: $a = 0.0631$ and $b = 0.000$ for **I**, $a = 0.0421$ and $b = 0.000$ for **II**, $a = 0.0811$ and $b = 4.67$ for **III**, $a = 0.0314$ and $b = 10.40$ for **IV**, $a = 0.0273$ and $b = 29.15$ for **V**, $a = 0.0328$ and $b = 3.45$ for **VI**, and $a = 0.0504$ and $b = 26.6807$ for **VII**.

mmol) were mixed with a starting composition of 3 Ag/8 Na/4 Ge/12 Se to give orange crystals of **I**. Finally, we rationalized the synthesis to systematically vary the concentration of Ag by varying the Ag/Na ratio while keeping the ratio of Ge/Se fixed at 4:10 (Table 1). A cursory glance at Table 1 indicates interesting findings: the concentration of the Ag^+ in the final structure does not obey a linear or proportional relationship with the starting Ag/Na ratio. When the amount of Ag is smaller than Ag/Na = 1:7 in the starting composition, $Ag_xNa_{(8-x)}Ge_4Se_{10}$ did not form; instead, we found another pseudoquaternary species, $Ag_{1.76}Na_{4.24}Ge_2Se_7$ (**VII**), related to $Na_6Ge_2Se_7$.[7]

Metathesis Route. To gain better control of the Ag^+ concentration in the final product, we sought to employ a metathesis route. There are two polymorphs of $Na_8Ge_4Se_{10}$, one of them has a 5-membered ring $Ge_4Se_{10}^{8-}$ unit[11] (referred to as $Na_8Ge_4Se_{10}$-5M), while the other contains the 6-membered chair form of the $Ge_4Se_{10}^{8-}$ unit[9b] (referred to as $Na_8Ge_4Se_{10}$-6M) as shown in Figure 1. The oxidation state of Ge is formally +3 in the two polymorphs. Both $Na_8Ge_4Se_{10}$-5M and $Na_8Ge_4Se_{10}$-6M can be prepared similarly by heating stoichiometric amounts of the elements at lower and higher temperatures, respectively. In the metathesis route, $Na_8Ge_4Se_{10}$-5M was reacted with AgCl in different ratios so that the equivalent amount of Ag^+ ion would substitute the Na^+ in $Na_8Ge_4Se_{10}$-5M and at the same time the 5-membered Ge_4Se_{10} unit was expected to rearrange to the 6-membered chair form at higher temperature and longer time forming the structure of $Ag_xNa_{(8-x)}Ge_4Se_{10}$ with the desired composition. Several reactions of $Na_8Ge_4Se_{10}$-5M and AgCl indicated that when the ratio of AgCl/$Na_8Ge_4Se_{10}$-5M was 1:1 or below, there was no Ag^+ substitution; moreover $Na_8Ge_4Se_{10}$-5M did transform to $Na_8Ge_4Se_{10}$-6M. However, when the ratio was 2:1, we observed Ag^+ substitution in transformed $Na_8Ge_4Se_{10}$-6M leading to **III**; 75.8 mg of $Na_8Ge_4Se_{10}$-5M (0.06 mmol) and 17.2 mg of AgCl (0.12 mmol) were loaded in a graphitized quartz ampule and sealed as described previously. The furnace was ramped to 825 °C at a rate of 35 °C/h, and the temperature was held constant at 825 °C for 96 h. The furnace was then slowly cooled to ambient temperature at a rate of 5 °C/h, and the orange crystals were recovered similarly as described previously. The

composition of the orange crystals of **III** was derived from the single-crystal data. The PXRD indicated the formation of pure **III** with no side product.

Single-Crystal X-ray Diffraction. Intensity data sets for the compounds (**I**−**VII**) were collected on a Bruker Smart CCD diffractometer. These data were integrated with SAINT;[18] the program SADABS was used for absorption correction.[19] The structures were solved by direct methods using SHELXS-97[20] and difference Fourier syntheses. Full-matrix least-squares refinement against $|F^2|$ was carried out using the SHELXTL-PLUS[21] suit of programs. For the compounds **I**−**VI**, the Se and Ge positions, which constitute half of the chairlike Ge_4Se_{10} units, were easily located. In the next cycle of refinement, the remaining six peaks with the electron densities between 48 and 28 e^-/site, were assigned as Na atoms. The refinement brought down the R1 value to 10%, but the thermal parameters for two Na atoms (Na1 and Na2), which initially had higher electron-density peaks (47.8 and 40.7 e^-/site), were unacceptably low. Moreover, the Na−Se bond distances for Na 1 and Na2 were shorter (2.8−2.9 Å) compared to other Na−Se distances (2.98−3.2 Å). This led us to believe that Na1 and Na2 could be Ag atoms or jointly occupied by Ag and Na. The refinement with Ag alone increased the R1 value to 14%, and the thermal parameters for all other atoms except Ag1 and Ag2 decreased to an unacceptable low. Finally those two sites were refined by putting both Na and Ag jointly, keeping their coordinates same while freely refining their occupancies. For compound **VII**, Ge, Se, and one Ag atom were easily located, where Ge and Se atoms make half of the corner-shared tetrahedral dimer Ge_2Se_7. Out of the three remaining peaks, two could be definitely refined as Na atoms, while the one with an electron density of 38 e^-/site and bond distances to the Se atoms in the range of 2.7−3 Å created a situation similar to that seen in **I**−**VI**; therefore, it was also refined with the mixed occupancy of Na and Ag, keeping the coordinates the same while freely varying the occupancies. The last cycles of refinement for **I**−**VII** included anisotropic thermal parameter refinement for all the atoms. Details of the final refinements and the cell parameters for **I**−**VII** are given in Table 2. The final atomic coordinates for **I** and the refined occupancies for the constitutionally disordered Na and Ag sites for **I**−**VI** are given in Table 3. The atomic coordinates for the new compound **VII** are given in Table 4.

Raman Spectroscopy. The bulk solid-state Raman spectra of compounds **II** and $Na_8Ge_4Se_{10}$-6M were collected on a Nicolet Magna-IR 760 spectrometer with a FT-Raman Module attachment by use of a Nd:YAG excitation laser (1064 nm).

UV−**vis Spectroscopy.** Diffuse reflectance measurements were taken on a Varian Cary 500 Scan UV−vis-NIR spectrophotometer equipped with a Praying Mantis accessory. A poly-Teflon standard was used as a reference. The Kubelka−Munk function was applied to obtain band gap information.[22]

Results and Discussion

Structure Description of $Ag_xNa_{(8-x)}Ge_4Se_{10}$. The series of compounds, denoted by $Ag_xNa_{(8-x)}Ge_4Se_{10}$ ($x = 0.31, 0.67, 0.77, 0.87, 1.05, 1.09$), **I**−**VI**, are topologically identical to their pure Na analogue, the $Na_8Ge_4Se_{10}$-6M structure but belong to a higher symmetry system. The isostructural compounds **I**−**VI**, differ only in their Ag content and crystallize in a centrosymmetric monoclinic space group *C*2/*c* (Table 2), while $Na_8Ge_4Se_{10}$-6M crystallizes in a triclinic system.

The structure of $Na_8Ge_4Se_{10}$-6M features a discrete anionic chairlike $Ge_4Se_{10}^{8-}$ unit interacting ionically with Na^+ cations, while the Ag-substituted phases (**I**−**VI**) reported here represent three-dimensional (3-D) structures because of more covalent-like Ag−Se bonds, containing channels filled with Na^+ cations. The 3-D structure of **I**−**VI** contains an anionic network of $[Ag_xNa_{4-x}Ge_4Se_{10}]^{4-}$ formed by predominantly covalent Ag/Na−Se layers cross-linked by Ge_4Se_{10} units via bridging Se-atoms. Only Na^+ cations occupy the channels formed by such cross-linking of Ag/Na−Se layers (Figure 2). The structure of **I**−**VI** can be more conveniently described in terms of packing of anions (Se^{2-}). Selenium anions form an approximately cubic close-packed array in which octahedral sites are occupied by Na^+/Ag^+, Na^+, and

Table 3. Atomic Coordinates ($\times 10^4$) and Equivalent Isotropic Displacement Parameters (Å^2 $\times$ 10^3) for **I** and Site Occupancy Factors (SOF) of Constitutionally Disordered Na and Ag Atoms in Compounds **I**−**VI**

atoms	Wyckoff	*x*	*y*	*z*	U_{eq}[a]
Ge(1)	8*f*	1374(2)	5483(1)	7318(1)	13(1)
Ge(2)	8*f*	1359(2)	3486(1)	7295(1)	15(1)
Se(1)	8*f*	1350(2)	6364(1)	6259(1)	21(1)
Se(2)	8*f*	3690(2)	5498(1)	8727(1)	20(1)
Se(3)	8*f*	1319(1)	4496(1)	6309(1)	16(1)
Se(4)	8*f*	3710(2)	3447(1)	8686(1)	19(1)
Se(5)	8*f*	1251(1)	2614(1)	6199(1)	18(1)
Na(1)	8*f*	2467(5)	4443(2)	9793(3)	38(2)
Ag(1)	8*f*	2467(5)	4443(2)	9793(3)	38(2)
Na(2)	8*f*	2292(6)	6495(2)	9796(3)	43(2)
Ag(2)	8*f*	2292(6)	6495(2)	9796(3)	43(2)
Na(3)	4*c*	2500	7500	5000	31(2)
Na(4)	4*e*	5000	4477(3)	7500	23(2)
Na(5)	4*e*	5000	6582(3)	7500	23(2)
Na(6)	4*e*	5000	2399(3)	7500	35(2)

atoms	**I**	**II**	**III**	**IV**	**V**	**VI**
Na(1)	0.909(5)	0.802(3)	0.784(5)	0.754(3)	0.710(4)	0.699(3)
Ag(1)	0.091(5)	0.198(3)	0.216(5)	0.246(3)	0.290(4)	0.301(3)
Na(2)	0.935(5)	0.862(2)	0.834(4)	0.811(3)	0.765(4)	0.758(3)
Ag(2)	0.065(5)	0.138(2)	0.166(4)	0.189(3)	0.235(4)	0.242(3)

[a] U_{eq} is defined as one-third of the trace of the orthogonalized U_{ij} tensor.

Table 4. Atomic Coordinates ($\times 10^4$) and Equivalent Isotropic Displacement Parameters (Å^2 $\times 10^3$) for **VII**

atoms	Wyckoff	*x*	*y*	*z*	*U*(eq)[a]	SOF
Ge(1)	8*f*	1600(1)	4233(1)	3568(1)	28(1)	
Se(1)	8*f*	3638(2)	3836(1)	3050(1)	56(1)	
Se(2)	8*f*	667(1)	2333(1)	3962(1)	31(1)	
Se(3)	8*f*	2013(1)	5736(1)	4724(1)	38(1)	
Se(4)	4*e*	0	5467(2)	2500	45(1)	
Ag(1)	4*e*	0	895(1)	2500	56(1)	
Na(2)	8*f*	−2210(2)	2575(2)	3563(1)	53(1)	0.62
Ag(2)	8*f*	−2210(2)	2575(2)	3563(1)	53(1)	0.38
Na(3)	4*a*	5000	5000	5000	48(2)	
Na(4)	8*f*	3811(5)	1395(5)	4140(4)	54(1)	

[a] U_{eq} is defined as one-third of the trace of the orthogonalized U_{ij} tensor.

(18) *SAINT, Data processing software for the SMART system*; Bruker Analytical X-ray Instruments, Inc.: Madison, WI, 1995.
(19) Sheldrick, G. M. *SADABS*; University of Göttingen: Göttingen, Germany, 1997.
(20) Sheldrick, G. M. *SHELXS-97, Programs for X-ray Crystal Structure Solution*; University of Göttingen: Göttingen, Germany, 1997.
(21) Sheldrick, G. M. *SHELXL-97, Programs for X-ray Crystal Structure Refinement*; University of Göttingen: Göttingen, Germany, 1997.
(22) (a) Wendlandt, W. W.; Hecht, H. G. *Reflectance Spectroscopy*; Interscience Publishers: New York, 1966. (b) Kotum, G. *Reflectance Spectroscopy*; Springer-Verlag: New York, 1969.

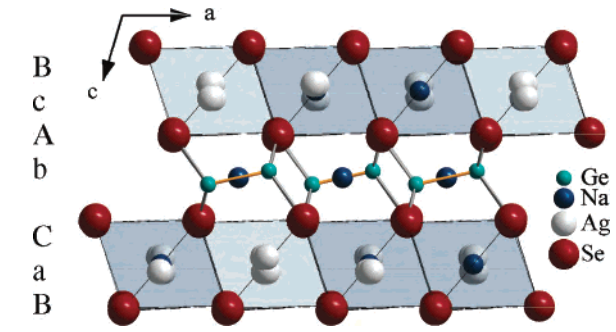

Figure 2. Perspective view of the 3-D structure of $Ag_xNa_{(8-x)}Ge_4Se_{10}$ along the *b* axis.

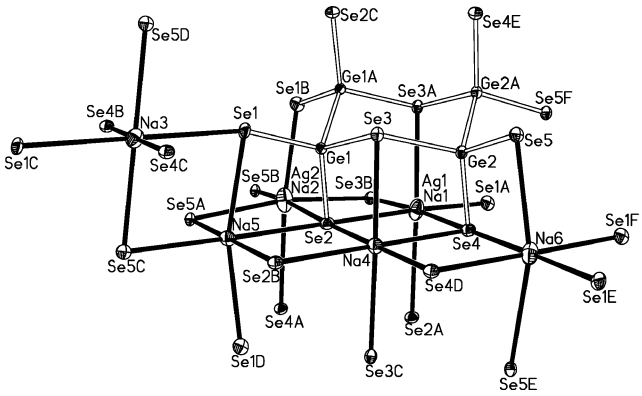

Figure 3. View of a part of the structure of **I** containing the asymmetric unit, showing the chairlike Ge_4Se_{10} unit (open full line). The thermal ellipsoids are given at 40% probability.

Ge_2^{6+} cations. If the Ge_2^{6+} cation is considered as one complex cation, then the centers of the Ge_2^{6+} units are actually located in the octahedral hole. The three successive cubic close-packed Se layers can be denoted as layers A, B, and C and their stacking as ABCABC; also the layers that form by filling the octahedral holes between the A and B, B and C, and C and A layers can be denoted as c, a, and b layers, respectively. The manner of occupancy of octahedral sites in between the Se layers, that is, c, a, b layers, is quite different. For example, octahedral layers containing Na^+ (Na4−Na6) and Ge_2^{6+} cations (e.g., in layers c and b) alternate with the layers that contain pure Na^+ (Na3) and mixed Ag^+/Na^+ cations (Ag1/Na1, Ag2/Na2) (e.g., in layer a). In the layers that contain both Na^+ and Ge_2^{6+} cations in the octahedral holes, 3/5 of the octahedral sites are occupied by Na^+ cations and 2/5 of the octahedral sites are occupied by Ge_2^{6+} cations, where Ge−Ge bonds are almost parallel to the Se layers.

As the structures of **I**−**VI** are identical and only differ in their Ag content, we will discuss the structure of **I** in detail. The asymmetric unit of **I** contains atoms in 13 distinct sites of which two Ge and five Se atoms constitute half of the Ge_4Se_{10} chairlike unit (Figure 3). Na and Ag jointly occupy two constitutionally disordered sites (Na1/Ag1 and Na2/Ag2) and their occupancies vary in structures **I**−**VI** (See Table 3), while Na atoms reside on special positions related by an inversion center (Na3) and a 2-fold symmetry axis (Na4−Na6). Each Ge atom forms one Ge−Ge bond to its symmetry-generated Ge atom and three Ge−Se bonds to two distinct Se atoms and one common Se atom (Se3). The Ge−Ge connectivity creates an ethane-like dimer, which is then connected by a bridging Se3 atom to form the chairlike Ge_4Se_{10} unit (Figure 3). The Ge−Se and Ge−Ge bond lengths are in the range of 2.313(2)−2.457(3) and 2.420(2)−2.427(3) Å, respectively, and Se−Ge−Se and Ge−Ge−Se bond angles are in the range of 104.83(6)−113.86(7) and 104.77(5)−113.06(8)°, respectively. These geometrical parameters are largely unaffected by the amount of Ag substitution in **I**−**VI** (See Supporting information, Table S1). All the Na/Ag and unique Na atom sites adopt octahedral coordination surrounded by six Se atoms. The Na/Ag−Se bond lengths are in the range of 2.887(4)−3.329(4) Å for Na1/Ag1 [$d(\text{Na1/Ag1−Se})_{av}$ = 3.059(6) Å] and 2.919(4)−3.348(5) Å for Na2/Ag2 [$d(\text{Na2/Ag2−Se})_{av}$ = 3.063(3) Å], while the Na−Se bond lengths are in the range of 3.0039(3)−3.1879(3) Å for Na3 [$d(\text{Na3−Se})_{av}$ = 3.0789(6) Å], 2.9862(4)−3.059(4) Å for Na4 [$d(\text{Na4−Se})_{av}$ = 3.0234(2) Å], 3.018(7)−3.146(5) Å for Na5 [$d(\text{Na5−Se})_{av}$ = 3.0943(3) Å], and 3.051(5)−3.1082(6) Å for Na6 [$d(\text{Na6−Se})_{av}$ = 3.059(6) Å] for compound **I**. It should be noted that although the average bond lengths of all the Na/Ag−Se and Na−Se bonds appear similar, there exists a greater difference between the shortest and the longest bonds in the cases of Na1/Ag1, Na2/Ag2, and Na3 (layer a cations), indicating more irregular octahedra compared to Na4−Na6 (cations in layers b and c). More importantly, this irregularity increases at the Na1/Ag1 and Na2/Ag2 sites as more silver is substituted, comparing compounds **I** through **VI**. For example, in **VI**, the shortest and the longest Na/Ag−Se distances at the Na1/Ag1 site are 2.875(4) and 3.3911(5) Å, respectively, while at the Na2/Ag2 site, they are 2.7946(9) and 3.5567(5) Å, respectively. Similar variations of *cis*- and *trans*-Se−Na/Ag−Se bond angles are also evident as a function of silver substitution. However, the Na−Se bonds and Se−Na−Se bond angles for sites Na3, Na4, and Na6 do not show significant variation across the solid solution, while Se−Na−Se bond angles at Na5 site does show little variation across the solid solution. The Na/Ag−Se bond lengths are slightly longer than pure Ag−Se bond lengths, where Ag is in octahedral coordination.[23] Relevant bond lengths and angles for compounds **I**−**VI** are given in Table 5.

Structural Phase Transition. The structure of $Na_8Ge_4Se_{10}$-6M, reported by Eisenmann et al.[9b] crystallizes in the space group $P\bar{1}$ with the cell parameters of a = 7.074(5) Å, b = 8.098(5) Å, c = 10.657(6) Å, α = 73.44(15)°, β = 70.84(15)°, γ = 81.73(15)°. Substitution of silver in $Na_8Ge_4Se_{10}$-6M leads to a structural phase transition from $P\bar{1}$ to $C2/c$ in $Ag_xNa_{8-x}Ge_4Se_{10}$. We do not have a complete solid solution between $Na_8Ge_4Se_{10}$-6M and $Ag_8Ge_4Se_{10}$ because the existence of the later compound is not known and a maximum of 13.625% Ag^+ could only be substituted for Na^+. We also could not establish the exact composition at which the $P\bar{1}$ to $C2/c$ phase transition occurs because our efforts to substitute a minimum amount of Ag^+ failed because of phase separation leading to a different Ag-substituted

(23) (a) Pfeiff, R.; Kniep, R. *J. Alloys Compd.* **1992**, *186*, 111. (b) Huang, F. Q.; Ibers, J. *Inorg. Chem.* **2001**, *40*, 865.

Table 5. Selected Bond Distances (Å) and Angles (deg) for the Compounds **I**−**VI**[a]

	I	**II**	**III**	**IV**	**V**	**VI**
Se(1)−Ag(1)/Na(1)$^{\#2}$	2.958(4)	2.9426(14)	2.949(2)	2.9279(17)	2.921(2)	2.9225(15)
Se(2)−Na(1)/Ag(1)	2.927(4)	2.9048(14)	2.898(2)	2.8946(17)	2.880(2)	2.8750(14)
Se(2)−Na(1)/Ag(1)$^{\#4}$	3.229(4)	3.2909(17)	3.317(3)	3.322(2)	3.344(2)	3.3458(17)
Se(3)−Ag(1)/Na(1)$^{\#1}$	3.028(4)	2.9978(16)	2.984(3)	2.986(2)	2.974(2)	2.9750(16)
Se(3)−Na(1)/Ag(1)$^{\#2}$	3.329(4)	3.3800(15)	3.374(3)	3.3944(18)	3.394(2)	3.3911(15)
Se(4)−Na(1)/Ag(1)	2.887(4)	2.8336(15)	2.821(3)	2.8103(17)	2.792(2)	2.7908(14)
Se(1)−Ag(2)/Na(2)$^{\#1}$	2.921(5)	2.8534(19)	2.839(4)	2.820(2)	2.796(3)	2.7946(19)
Se(2)−Na(2)/Ag(2)	2.919(4)	2.8954(15)	2.882(3)	2.8771(18)	2.859(2)	2.8605(15)
Se(3)−Na(2)/Ag(2)$^{\#2}$	3.173(4)	3.1668(16)	3.176(3)	3.1636(19)	3.159(2)	3.1623(15)
Se(4)−Na(2)/Ag(2)$^{\#4}$	3.348(5)	3.457(2)	3.477(4)	3.513(2)	3.550(2)	3.5567(15)
Se(5)−Ag(2)/Na(2)$^{\#2}$	2.959(4)	2.9461(16)	2.948(3)	2.9394(19)	2.929(2)	2.9258(16)
Se(5)−Na(2)/Ag(2)$^{\#5}$	3.058(4)	3.0568(15)	3.046(3)	3.0571(19)	3.052(2)	3.0490(15)
Se(4)−Na(1)−Se(2)	90.58(11)	92.14(4)	92.70(8)	92.76(5)	93.40(6)	93.53(4)
Se(4)−Na(1)−Se(1)$^{\#7}$	102.34(12)	102.93(4)	102.41(7)	103.17(5)	102.95(6)	102.76(4)
Se(2)−Na(1)−Se(1)$^{\#7}$	165.60(16)	162.36(6)	161.78(11)	160.94(7)	159.94(7)	159.92(6)
Se(4)−Na(1)−Se(3)$^{\#1}$	101.77(13)	103.95(5)	104.75(9)	104.87(6)	105.64(6)	105.71(5)
Se(2)−Na(1)−Se(3)$^{\#1}$	98.73(12)	99.78(4)	100.26(8)	100.13(5)	100.58(6)	100.69(4)
Se(1)$^{\#7}$−Na(1)−Se(3)$^{\#1}$	84.99(10)	85.59(4)	85.83(7)	85.99(5)	86.28(5)	86.26(4)
Se(4)−Na(1)−Se(2)$^{\#4}$	87.40(11)	87.00(4)	86.39(7)	86.68(5)	86.15(5)	86.07(4)
Se(2)−Na(1)−Se(2)$^{\#4}$	84.29(10)	82.81(4)	82.60(7)	82.17(5)	81.67(5)	81.65(4)
Se(1)$^{\#7}$−Na(1)−Se(2)$^{\#4}$	89.90(11)	88.80(4)	88.19(7)	88.30(5)	87.83(6)	87.76(4)
Se(3)$^{\#1}$−Na(1)−Se(2)$^{\#4}$	170.27(15)	168.57(5)	168.26(9)	168.03(6)	167.75(6)	167.73(5)
Se(4)−Na(1)−Se(3)$^{\#7}$	173.23(15)	171.68(6)	170.60(10)	170.91(7)	170.09(7)	169.96(6)
Se(2)−Na(1)−Se(3)$^{\#7}$	93.25(11)	91.23(4)	91.02(7)	90.33(5)	89.67(6)	89.72(4)
Se(1)$^{\#7}$−Na(1)−Se(3)$^{\#7}$	73.28(9)	72.64(4)	72.55(6)	72.39(4)	72.33(5)	72.32(3)
Se(3)$^{\#1}$−Na(1)−Se(3)$^{\#7}$	83.18(10)	82.95(3)	83.05(6)	82.97(4)	83.01(5)	82.96(4)
Se(2)$^{\#4}$−Na(1)−Se(3)$^{\#7}$	87.42(11)	85.88(4)	85.53(7)	85.28(5)	84.97(5)	85.01(4)
Se(2)−Na(2)−Se(1)$^{\#1}$	99.11(13)	101.41(5)	102.00(10)	102.60(7)	103.55(7)	103.67(5)
Se(2)−Na(2)−Se(5)$^{\#7}$	169.82(19)	166.55(7)	165.56(13)	164.82(9)	163.39(9)	163.11(7)
Se(1)$^{\#1}$−Na(2)−Se(5)$^{\#7}$	87.60(12)	88.83(4)	89.10(8)	89.43(6)	89.90(6)	90.02(5)
Se(2)−Na(2)−Se(5)$^{\#8}$	91.00(12)	91.93(4)	92.14(8)	92.41(5)	92.71(6)	92.76(5)
Se(1)$^{\#1}$−Na(2)−Se(5)$^{\#8}$	107.36(15)	109.98(6)	110.44(10)	111.33(7)	112.20(7)	112.37(6)
Se(5)$^{\#7}$−Na(2)−Se(5)$^{\#8}$	94.31(11)	92.74(4)	92.57(7)	91.75(5)	91.09(6)	91.05(4)
Se(2)−Na(2)−Se(3)$^{\#7}$	96.73(11)	95.86(4)	95.44(7)	95.44(5)	94.92(6)	94.71(4)
Se(1)$^{\#1}$−Na(2)−Se(3)$^{\#7}$	83.05(11)	84.03(4)	84.20(8)	84.55(5)	84.97(6)	84.96(4)
Se(5)$^{\#7}$−Na(2)−Se(3)$^{\#7}$	76.37(10)	76.36(4)	76.33(7)	76.29(5)	76.37(6)	76.43(4)
Se(5)$^{\#8}$−Na(2)−Se(3)$^{\#7}$	165.95(17)	162.32(7)	161.74(12)	160.29(8)	158.98(8)	158.88(7)
Se(2)−Na(2)−Se(4)$^{\#4}$	84.68(12)	82.97(4)	82.50(8)	82.14(5)	81.35(4)	81.15(3)
Se(1)$^{\#1}$−Na(2)−Se(4)$^{\#4}$	170.96(16)	169.87(6)	169.55(10)	169.27(7)	168.91(2)	168.85(6)
Se(5)$^{\#7}$−Na(2)−Se(4)$^{\#4}$	87.61(12)	85.57(5)	85.07(8)	84.50(6)	83.75(2)	83.687(4)
Se(5)$^{\#8}$−Na(2)−Se(4)$^{\#4}$	80.66(11)	78.77(4)	78.54(7)	77.78(5)	77.11(6)	77.054(3)
Se(3)$^{\#7}$−Na(2)−Se(4)$^{\#4}$	88.37(12)	86.45(5)	85.99(8)	85.41(5)	84.69(2)	84.62(3)

[a] Symmetry transformations used to generate equivalent atoms: #1 $-x, y, -z + 3/2$; #2 $x, -y + 1, z - 1/2$; #4 $-x + 1, -y + 1, -z + 2$; #5 $-x + 1/2, y - 1/2, -z + 3/2$; #7 $x, -y + 1, z + 1/2$; #8 $-x + 1/2, y + 1/2, -z + 3/2$.

structure, $Ag_{1.76}Na_{4.24}Ge_2Se_7$ (**VII**). This finding can also be indicative of the fact that silver-substituted *triclinic* $Na_8Ge_4Se_{10}$-6M may not exist. So, we will compare the structure of $Na_8Ge_4Se_{10}$-6M with the structure of $Ag_xNa_{8-x}Ge_4Se_{10}$ and try to describe what may be the driving force of the transition by reviewing the microscopic structural distortions. The asymmetric unit of $Na_8Ge_4Se_{10}$-6M contains 5 Na^+ cations; two of them (Na2, Na3) sit on special positions related by a center of inversion, while Na1, Na4, and Na5 occupy general positions (this numbering scheme is same as that reported by Eisenmann et al.).[9b] The rest of the asymmetric unit is same as **I**−**VI**. Complementary views of the structures of both compounds are shown in Figure 4a and b. The monoclinic structure, when viewed as triclinic, gives "triclinic" cell parameters wherein the *a*, *b*, and *c* axes are equivalent to the *b*, *c*, and *double a* axes of $Na_8Ge_4Se_{10}$-6M. Na1, Na3, and Na4 fill all the octahedral sites of the layer a in $Na_8Ge_4Se_{10}$-6M, while Na2, Na5, and Ge_2^{6+} cations fill the octahedral sites in the alternate layers (layer c and b), which host the Ge_4Se_{10} unit. Although the count of Na^+ ions and their numbering schemes are different in $Na_8Ge_4Se_{10}$-6M and $Ag_xNa_{8-x}Ge_4Se_{10}$, it is not hard to determine the equivalence of any one Na^+ ion in the other. For example Na1, Na4, Na3, and Na2 of $Na_8Ge_4Se_{10}$-6M are equivalent to Na1, Na2, Na3, and Na4, respectively, of $Ag_xNa_{8-x}Ge_4Se_{10}$, while Na5 of $Na_8Ge_4Se_{10}$-6M splits into Na5 and Na6 in $Ag_xNa_{8-x}Ge_4Se_{10}$. It is evident that Ag substitution takes place only at the Na1 and Na4 sites of $Na_8Ge_4Se_{10}$-6M (which are Na1/Ag1 and Na2/Ag2, respectively, in $Ag_xNa_{8-x}Ge_4Se_{10}$) and the Na3 site remains unchanged.

Another visible change is noticed in the orientation of the Ge−Ge bonds of the Ge_4Se_{10} unit; a building block that is perpendicular to the Se layers in $Na_8Ge_4Se_{10}$-6M becomes almost parallel upon Ag substitution (**I**−**VI**), Figures 2 and 4.

A relevant question is why silver substitution takes place in the octahedral sites of the pure Na^+ layers (a, c′, and b′ layers) in $Na_8Ge_4Se_{10}$-6M but not in the others (c, b, and a′ layers). The answer probably lies in the distortions of the octahedra, which can be quantified by continuous symmetry measurement analysis according to Zabrodsky et al., Ok et

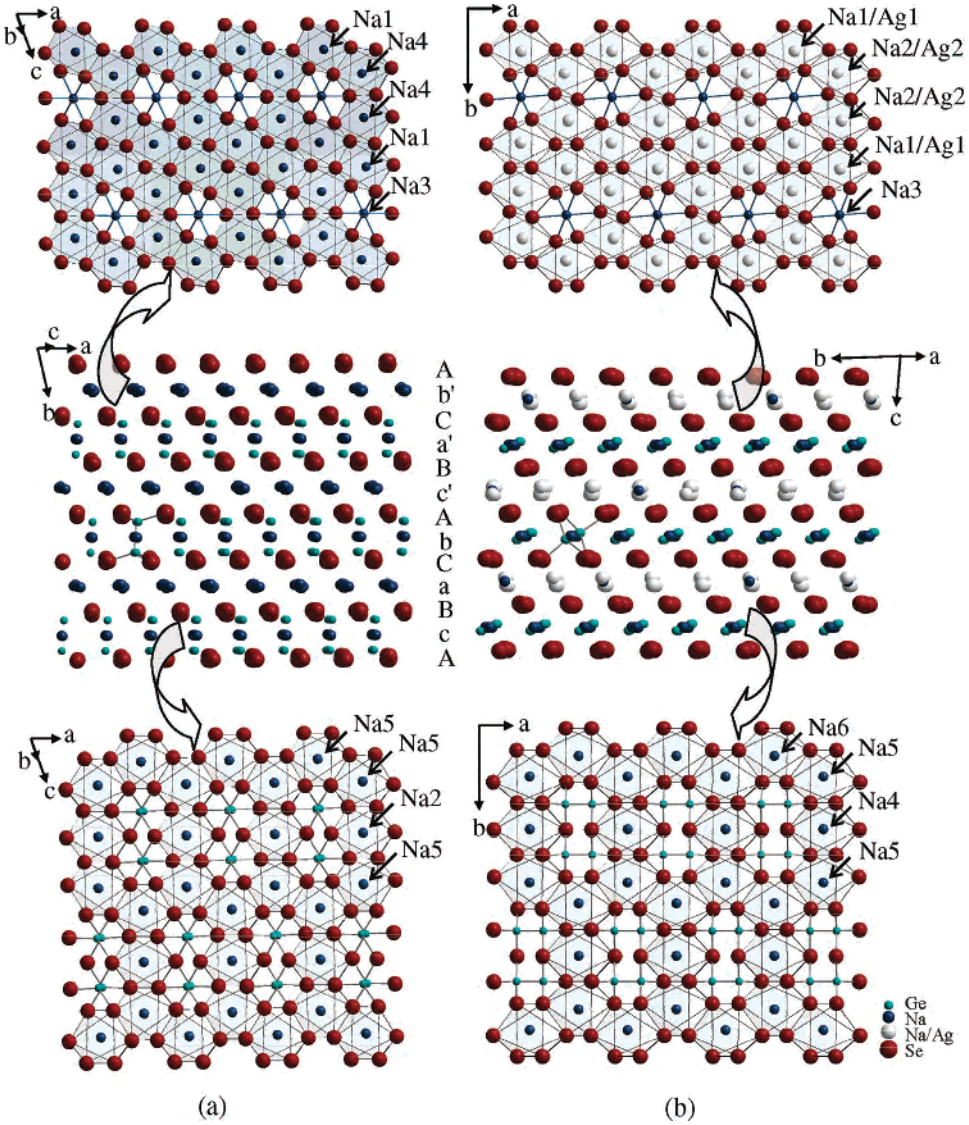

Figure 4. (a) Views of the different close-packed layers of $Na_8Ge_4Se_{10}$-6M (top, layer a, c′, or b′ cations) down the *b* axis and the layers containing the Ge_4Se_{10} building blocks (bottom, layer b, c, or a′ cations). The middle figure shows the view parallel to the layers. A, B, and C indicate the stacking of the cubic close-packed Se layers, while the lower-case letters (c, a, b, etc.) indicate stacking of the cation layers. (b) Complementary views of the Ag-substituted phases (**I**−**VI**) oriented similarly to those in part a.

al., and Alvarez et al.[24] The basic idea behind this analysis of octahedral distortion is to "*quantify the minimal distance movement that the points of an object have to undergo in order to be transformed into a shape of the desired symmetry*".[24a] In our case this means, we superimpose a perfect octahedron over the existing distorted one and measure the distance between the six ligands of the distorted octahedron and the six vertices of the perfect platonic octahedron. To find the positions of the six ligands (P0−P5) in a "perfect" octahedra all the cis angles between ligand atoms (P0−P5), central atom (Z), and ligand atoms have to be 90°, and the three trans angles must be 180° (Figure 5). Subsequently, the perfect polyhedron has to be normalized to the size of the distorted one, that is, the size of the distorted object has to be scaled so that the longest distance between the central atom (Z) and any of the ligands (D0−D5) in the "distorted" octahedra is 1. All distances may be averaged, and this average becomes the distance between Z and the perfect vertices P0−P5. To quantify the minimal distance distortions and get a value for the distortion of a given $[ZD_6]$ unit, one calculates the continuous symmetry measure $S_{(sym)}$, which is the average square of the transitions D_i to P_i (keeping in mind that D_i and P_i are three-dimensional vectors and $|D_i - P_i|$ gives the length of a vector)

$$S_{(oct)} = 100 \frac{\sum_{i=0}^{5} |D_i - P_i|^2}{6} \qquad (1)$$

The factor of 100 is introduced only to have a value that is more convenient.[24a]

(24) (a) Zabrodsky, H.; Peleg, S.; Avnir, D. *J. Am. Chem. Soc.* **1992**, *114*, 7843. (b) Ok, K. M.; Halasyamani, P. S.; Casanova, D.; Llunell, M.; Alemany, P.; Alvarez, S. *Chem. Mater.* **2006**, *18*, 3176. (c) Alvarez, S.; Alemany, P.; Casanova, D.; Cirera, J.; Llunell, M.; Avnir, D. *Coord. Chem. Rev.* **2005**, *249*, 1693.

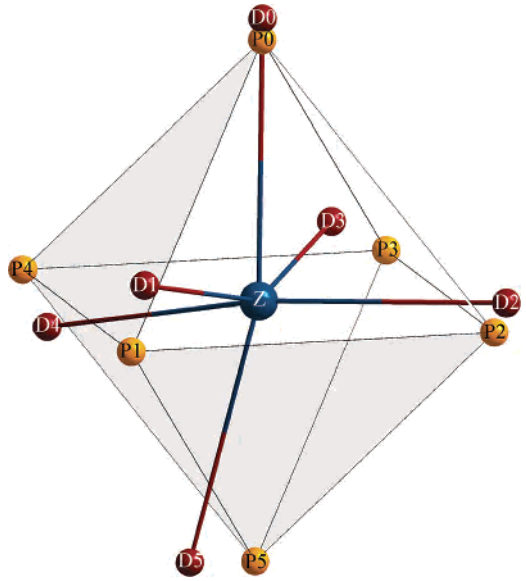

Figure 5. Schematic representation showing how a perfect octahedron (labeled P) is superimposed over a distorted octahedron (labeled D).

According to this equation, $S_{(oct)}$ can take values between 0 and 100. A value of $S_{(oct)} = 0$ represents a [ZD_6] unit that has the perfect octahedral symmetry, that is, the higher the value of $S_{(oct)}$, the more distorted the polyhedron.

It was found that the values of $S_{(oct)}$ for the cations in the pure Na layers (a, c′, and b′ layers) in $Na_8Ge_4Se_{10}$-6M are high [$S_{(oct)}$(Na1) = 3.5226, $S_{(oct)}$(Na3) = 2.2953, $S_{(oct)}$(Na4) = 5.483] relative to those in the alternate layers (c, b, and a′ layers) [$S_{(oct)}$(Na2) = 0.7093, $S_{(oct)}$(Na5) = 1.7694]. This clearly indicates that Ag prefers the more distorted Na1 and Na4 sites for substitution; these sites are labeled Na1/Ag1 and Na2/Ag2, respectively, in $Ag_xNa_{8-x}Ge_4Se_{10}$. For small amounts of Ag substitution as in **I** and formation of the monoclinic phase, the distortions at Na1/Ag1 and Na2/Ag2 drop immediately as indicated by their $S_{(oct)}$ values [$S_{(oct)}$(Na1/Ag1) = 2.5151 and $S_{(oct)}$(Na2/Ag2) = 3.1063], while the distortion at Na3 site drops as well ($S_{(oct)}$(Na3) = 1.0027) compared to the Ag-free phase. As more and more Ag incorporation takes place, the distortions at Na1/Ag1 and Na2/Ag2 sites increase linearly as a function of Ag incorporation, as shown in Figure 6, while distortion at the Na3 site remains invariant across the solid solution. Ag incorporation in the a, c′, and b′ layers induces a cooperative effect in the alternate layers (b, c, and a′ layers). For example, distortions at Na6 decrease, while distortions at the Na4 and Na5 sites increase when compared to their equivalent sites in the unsubstituted $Na_8Ge_4Se_{10}$-6M. However, the distortions at the Na4 and Na6 sites remain largely unaffected across the solid solutions (Figure 6), while there is an increase in the distortion at the Na5 site as a function of Ag incorporation, although it is less pronounced than that of Na1/Ag1 and Na2/Ag2. The distortions at the Na1/Ag1 and Na2/Ag2 sites do not belong to any classical type of distortions such as trigonal or tetragonal distortion. The distortions involve the compression at four Ag/Na−Se bonds and elongation at two Ag/Na−Se bonds, indicating that with more and more Ag substitution, the coordination of the Na1/Ag1 and Na2/

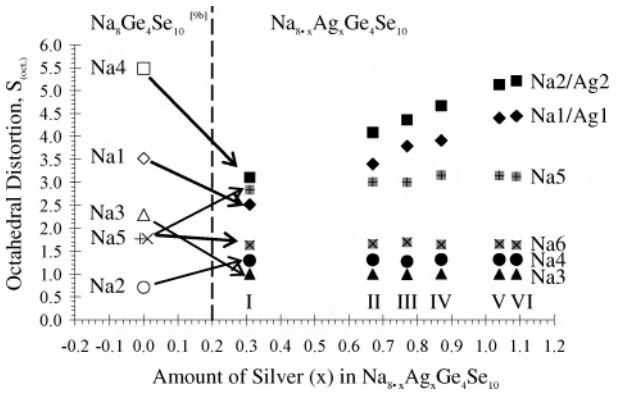

Figure 6. Plot of the degree of distortion, $S_{(oct)}$, of various octahedral sites in $Na_8Ge_4Se_{10}$-6M and $Ag_xNa_{(8-x)}Ge_4Se_{10}$ as a function of Ag substitution. The degree of distortion is calculated on the basis of continuous-symmetry measure analysis, eq 1. The open symbols correspond to the Na sites in pure $Na_8Ge_4Se_{10}$-6M, while the filled symbols correspond to the Na and Na/Ag sites in $Ag_xNa_{(8-x)}Ge_4Se_{10}$.

Ag2 sites tend toward four-coordinate. The four compressed Ag/Na−Se bonds tend to take the shape of a flattened tetrahedral geometry, often favored by Ag^+ surrounded by four chalcogen atoms.[25] In other words, Ag tends to force a flattened tetrahedral geometry because the shortening of the four bonds can be attributed to the more covalent Ag−Se character. There is a consistent decrease of the *c* axis length and volume as a function of Ag substitution. Such contractions are not surprising and increase as a function of the degree of covalence of the metal−ligand bonds.[26]

The distortions at Na1/Ag1 and Na2/Ag2 sites resulting from Ag substitution induce a distortion at the Na5 site, which increases slightly across the solid solution. Careful examination of the distortion at Na5 site reveals that *trans*-Se1−Na5−Se1 and Se5−Na6-Se5 angles, 163.2(2) and 164.0(2)°, respectively, for **I** deviate more from 180° than their equivalent angles in $Na_8Ge_4Se_{10}$-6M (167.38(2)°). While the *cis*-Se2−Na5−Se2 and Se4−Na6−Se4 angles, 92.03-(7) and 92.39(3)°, respectively, for **I** converge more toward 90° than their equivalent angles in $Na_8Ge_4Se_{10}$-6M (95.65-(2)°). Such deviation of the trans angles from 180° and convergence of cis angles toward 90° elongate the size of the two adjacent octahedral holes and the Ge−Ge bonds of the $Ge_4Se_{10}^{8-}$ may lie parallel to the Se layer (compare Figure 4, bottom left and right). Because of this change of the orientation of the Ge−Ge bonds there is a dramatic change of the symmetry of the Ge_4Se_{10} unit. In $Na_8Ge_4Se_{10}$-6M, $Ge_4Se_{10}^{8-}$ units were related by a center of inversion, while in $Ag_xNa_{8-x}Ge_4Se_{10}$ (**I**−**VI**), $Ge_4Se_{10}^{8-}$ units are related by a 2-fold rotation symmetry, and thus a higher symmetry is induced. The existence of distortions at Na1/Ag1 and Na2/Ag2 sites may be the result of a size mismatch or different coordination preference of Na and Ag atoms, while the twisting of the Ge−Ge bonds, a secondary process, may be responsible for the phase transition.

Végard's Law. The variation of structural parameters often reveals important insights and the most basic of these

(25) (a) Wachhold, M.; Kanatzidis, M. G. *Inorg. Chem.* **2000**, *39*, 2337. (b) Huang, F. Q.; Ibers, J. A. *J. Solid State Chem.* **2001**, *158*, 299. (c) Tampier, M.; Johrendt, D. *Z. Anorg. Allg. Chem.* **2001**, *627*, 312.
(26) Shannon, R. D.; Vincent, H. *Struct. Bonding* **1974**, *19*, 1.

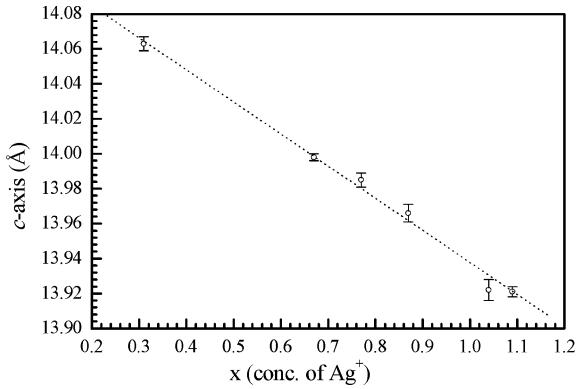

Figure 7. Plot of the variation of the *c* parameter in $Ag_xNa_{(8-x)}Ge_4Se_{10}$ [$x = 0.31$ (**I**), 0.67 (**II**), 0.77 (**III**), 0.87 (**IV**), 1.05 (**V**), 1.09 (**VI**)] with the concentration of Ag^+. The vertical line at each point is a measure of error in the third decimal. The dashed line indicates linear fit of the points.

is the change in the lattice parameters. The consistency of the solid solutions is often judged by the composition-dependent lattice parameter changes in terms of the empirical Végard's law.[27] This law states that in the absence of strong electronic effects, the variation of lattice parameters is linear with composition. As mentioned earlier, the length of the *c* axis and volume decrease with increasing Ag concentration (see Table 2). The plot of the *c* parameter against Ag concentration is given in Figure 7 indicating a linear dependence. There are two factors that control the linearity of the *c* parameters; the mismatch of size resulting from the difference in the ionic radii ($r_{Na^+}{}^{CN=6} = 1.02$, $r_{Ag^+}{}^{CN=6} = 1.15$)[28] between Na^+ and Ag^+ cations, as well as the degree of covalence. Here, a linear decrease rather than an increase is observed because of the increased covalence with increasing Ag concentration, which outweighs the effect of larger ionic radius of Ag^+.

Structure Description of $Ag_xNa_{(6-x)}Ge_2Se_7$ ($x = 1.76$). Unlike compounds **I**−**VI**, the structure of **VII** is isostructural to its pure Na analogue; $Na_6Ge_2Se_7$ and Ge atoms are formally assigned as Ge^{4+} ions. Both structures crystallize in the *C*2/*c* space group with nearly similar lattice parameters. The cell parameters for $Na_6Ge_2Se_7$ are as follows: $a = 9.451(4)$ Å, $b = 10.914(4)$ Å, $c = 15.874(6)$ Å, and $\beta = 104.7(1)°$.[7b] Careful examination reveals that Ag substitution in $Na_6Ge_2Se_7$ increases the *a* axis length while the *b* and *c* axis lengths are decreased; the β angle is also slightly contracted (see Table 2). The overall effect of these changes is a 3.87% reduction of the volume of the unit cell in **VII** compared to $Na_6Ge_2Se_7$, as well as the relative dimensionality of the structure, caused by the introduction of a more covalent Ag^+ cation. The structure of $Na_6Ge_2Se_7$ can be described in terms of discrete $Ge_2Se_7^{6-}$ anions packed with Na^+ cations through electrostatic forces. The structure of **VII**, on the other hand, can be described as a covalently connected 3-D network of $[Ag_{1.76}Na_{1.24}Ge_2Se_7]^{3-}$ possessing channels filled with Na^+ cations (Figure 8a). Ge_2Se_7 dimers are linked by $AgSe_4$ tetrahedra through corner-sharing to form a layer with apertures perpendicular to the *ab* plane (Figure 8b). Such layers are cross-linked by $Na/AgSe_4$ tetrahedra to form the 3-D anionic network. Na^+ cations occupy channels formed by such cross-linking.

The asymmetric unit of **VII** contains 9 unique sites, which are occupied by one Ge, four Se, one Ag, and two Na atoms, while both Na and Ag jointly occupy one of the sites (Na2/Ag2) (Figure 9). Ge1 is surrounded by four Se atoms in a tetrahedral environment. Ge−Se bond lengths are in the range of 2.3330(2)−2.337(5) Å [$d(Ge1-Se)_{av} = 2.343(6)$ Å], and the Se−Ge−Se bond angles are in the range of 96.90(6)−114.53(6)°, indicating a distorted tetrahedron. Ge1 is connected to two Na (Na3, Na4), one Ag (Ag1), and one Na/Ag (Na2/Ag2) atoms through Ge−Se−Na, Ge−Se−Ag, and Ge−Se−Na/Ag linkages, respectively, as well as to another symmetrically generated Ge atom through Se4, thereby forming a corner-shared $Ge_2Se_7^{6-}$ dimer. Both Ag1 and Na2/Ag2 are surrounded by 4 Se atoms in tetrahedral coordination. Ag1−Se bond lengths are in the range of 2.652(4)−2.769(6) Å [$d(Ag1-Se)_{av} = 2.710(5)$ Å], and Se−Ag1−Se bond angles are in the range of 76.73(6)−131.24(5)°. Na2/Ag2−Se bond lengths are in the range of 2.738(3)−3.130(2) Å [$d(Na2/Ag2-Se)_{av} = 2.893(2)$ Å], and Se−(Na2/Ag2)−Se bond angles are in the 81.05(6)−134.91(9)° range. Both bond lengths and bond angles indicate that $Ag1Se_4$ and $Na2/Ag2Se_4$ tetrahedra are fairly distorted. Na3 and Na4, on the other hand, are surrounded by six Se atoms in an octahedral environment. Na−Se bond lengths are in the range of 2.944(3)−3.212(4) [$d(Na3-Se)_{av} = 3.076(2)$ Å] and 3.048(5)−3.315(5) Å [$d(Na4-Se)_{av} = 3.107(3)$ Å] for Na3 and Na4, respectively. The *cis*- and *trans*-Se−Na−Se bond angles are in the range of 77.30(3)−94.54(3) and 180°, respectively, for Na3 and 75.83(2)−123.44(5) and 149.24(4)−167.7(2)°, respectively, for Na4. Both bond lengths and angles indicate that $Na4Se_6$ is more distorted than $Na3Se_6$. Ag−Se bond lengths are similar to those reported in the literature for Ag in tetrahedral coordination, while Na/Ag−Se bond lengths are slightly longer.[28] Selected geometrical parameters for compound **VII** are given in Table 6.

No Structural Phase Transition. As low as 3.87% substitution of Na^+ by Ag^+ in $Na_8Ge_4Se_{10}$-6M causes a phase transition in **I**, while 29.33% substitution of Na^+ by Ag^+ in $Na_6Ge_2Se_7$ does not cause any phase transition. At this point it is necessary to compare the microstructural distortions of **VII** with $Na_6Ge_2Se_7$. Unlike $Na_8Ge_4Se_{10}$-6M where all the Na^+ cations are in octahedral coordination, $Na_6Ge_2Se_7$ has Na^+ cations in three different coordination environments. One of them has a very flattened tetrahedral coordination; one has (1 + 1)-fold capped tetrahedral environment in (4 + 2) coordination with two long Na−Se bonds [3.427(3) and 3.540(2) Å], while two other Na^+ cations have octahedral environments (one almost regular and the other distorted). As we have seen in **I**−**VI**, Ag^+ cations substitute more distorted octahedral sites in $Na_8Ge_4Se_{10}$-6M and tend to become a flattened tetrahedral coordination with increased Ag-substitution. In $Na_6Ge_2Se_7$, there already exist two flattened tetrahedral Na^+ sites, so quite expectedly, Ag^+ cations fully substitute a very distorted (flattened) tetrahedral site, and partially substitute another (4 + 2) coordination

(27) (a) Vegard, L. *Z. Phys.* **1921**, *5*, 17. (b) Vegard, L. *Z. Kristallogr.* **1928**, *67*, 239.
(28) Shannon, R. D. *Acta Crystallogr.* **1976**, *A32*, 751.

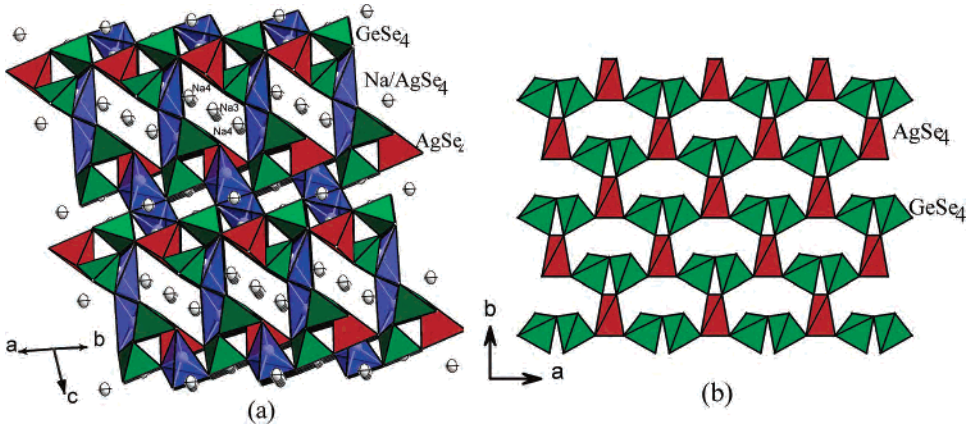

Figure 8. (a) Perspective view of the 3-D structure of **VII** approximately along the [1 1 1] direction. (b) Part of the 3-D structure of **VII** showing the layerlike architecture when viewed along the *c* axis.

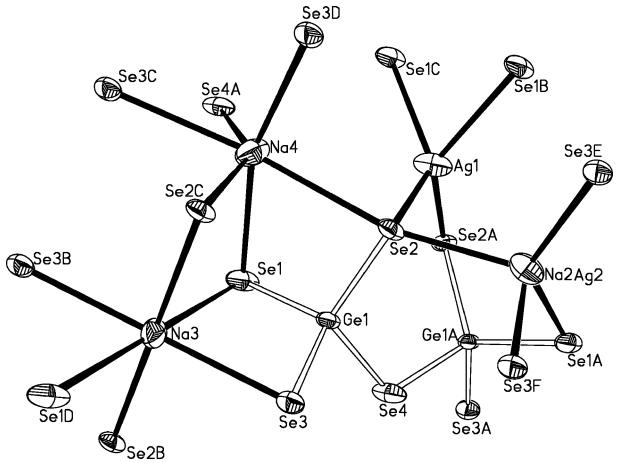

Figure 9. View of a part of the structure of **VII** containing the asymmetric unit, showing the corner-shared dimer of $GeSe_4$ tetrahedra ($Ge_2Se_7^{6-}$, in open full line). The thermal ellipsoids are given at 40% probability.

Table 6. Selected Bond Distances (Å) and Angles (deg) for the Compound **VII**[a]

Ge(1)−Se(1)	2.3300(16)	Se(1)−Ge(1)−Se(2)	110.01(6)
Ge(1)−Se(2)	2.3331(15)	Se(1)−Ge(1)−Se(3)	111.22(7)
Ge(1)−Se(3)	2.3364(15)	Se(2)−Ge(1)−Se(3)	113.53(6)
Ge(1)−Se(4)	2.3711(15)	Se(1)−Ge(1)−Se(4)	110.07(6)
Se(1)−Ag(1)$^{\#1}$	2.7692(16)	Se(2)−Ge(1)−Se(4)	114.53(6)
Se(2)−Ag(1)	2.6523(14)	Se(3)−Ge(1)−Se(4)	96.90(6)
Ag(1)−Se(1)$^{\#3}$	2.7692(16)	Se(2)−Ag(1)−Se(2)$^{\#2}$	110.23(7)
Ag(1)−Se(1)$^{\#8}$	2.7692(16)	Se(2)−Ag(1)−Se(1)$^{\#3}$	103.75(4)
Se(1)−Ag(2)/Na(2)$^{\#2}$	2.864(3)	Se(2)$^{\#2}$−Ag(1)−Se(1)$^{\#3}$	131.24(5)
Se(3)−Ag(2)/Na(2)$^{\#1}$	2.840(2)	Se(2)−Ag(1)−Se(1)$^{\#8}$	131.24(5)
Se(2)−Na(2)	2.738(3)	Se(2)$^{\#2}$−Ag(1)−Se(1)$^{\#8}$	103.75(4)
Se(3)−Na(2)$^{\#6}$	3.130(2)	Se(1)$^{\#3}$−Ag(1)−Se(1)$^{\#8}$	76.73(6)
		Se(2)−Na(2)−Se(3)$^{\#3}$	101.52(8)
		Se(2)−Na(2)−Se(1)$^{\#2}$	120.54(8)
		Se(3)$^{\#3}$−Na(2)−Se(1)$^{\#2}$	134.91(9)
		Se(2)−Na(2)−Se(3)$^{\#6}$	89.99(7)
		Se(3)$^{\#3}$−Na(2)−Se(3)$^{\#6}$	81.05(6)
		Se(1)$^{\#2}$−Na(2)−Se(3)$^{\#6}$	112.22(8)

[a] Symmetry transformations used to generate equivalent atoms: #1 $x + 1/2, y + 1/2, z$; #2 $-x, y, -z + 1/2$; #3 $x - 1/2, y - 1/2, z$; #6 $-x, -y + 1, -z + 1$; #8 $-x + 1/2, y - 1/2, -z + 1/2$.

site (can be best described as a distorted tetrahedral site ignoring two long bonds). The two longer Na−Se bonds of (4 + 2) coordination in unsubstituted $Na_6Ge_2Se_7$ becomes further elongated [3.598(2) and 4.135(2) Å] from the equivalent site (Na2/Ag2) in **VII** making it a four-coordinated tetrahedron with four shortened Na2/Ag2-Se bonds. Thus, the *a* axis is slightly lengthened, while the *b* and *c* axes are shortened, albeit no structural phase transition occurred. Clearly, more compositions with higher levels of Ag^+ substitution have to be synthesized to see any possible composition-dependent phase transition, but none have been seen in our hands. Such studies will reveal whether Ag^+ begins to fill the octahedral sites when all the tetrahedral sites are fully substituted or if another phase transition is found.

Site Preferences. It is important to consider the site preference of Ag^+ during the substitutions. Although we have found that Ag^+ preferentially substitutes for the more distorted Na^+ sites, when all the Na^+ ions are in octahedral coordination and tend to adopt a flattened tetrahedral coordination as the amount of Ag increases. However, it is still not clear if, given a choice, Ag would prefer a distorted tetrahedral site or a distorted octahedral Na-site when the degree of distortions are equivalent. Moreover, it is not clear if Ag^+ always prefers tetrahedral coordination over octahedral during substitution regardless of the degree of distortion. It has been reported that Ag^+ can actually tolerate a large degree of distortion in the tetrahedral coordination.[25] Recently, Wang and Lee also found that Ag^+ cations tend to substitute distorted tetrahedral In^{3+} sites over octahedral sites in $AgPb_8In_{17}S_{34}$.[29] Clearly, more experiments as well as theoretical studies are needed to understand the site preference during substitution.

Spectroscopy. The effect on optical properties resulting from Ag^+ substitution in $Na_8Ge_4Se_{10}$-6M was examined by analyzing and comparing the diffuse reflectance spectra of **II** with $Na_8Ge_4Se_{10}$-6M. The plot of the Kubelka−Munk function against the energy given in Figure 10 shows steep absorption edges expected for semiconducting compounds. The optical band gaps as derived from the extrapolation of the linear region of the absorption edges are 2.3 and 2.65 eV for **II** and $Na_8Ge_4Se_{10}$-6M, respectively, consistent with the observed color (orange for **II** and yellow for $Na_8Ge_4Se_{10}$-6M). The band gap values clearly indicate that there is a red shift because of Ag^+ substitution. Alkali cation electrons make no contributions around the Fermi level

(29) Wang, K.-C. Lee, C.-S. *Inorg. Chem.* **2006**, *45*, 1415.

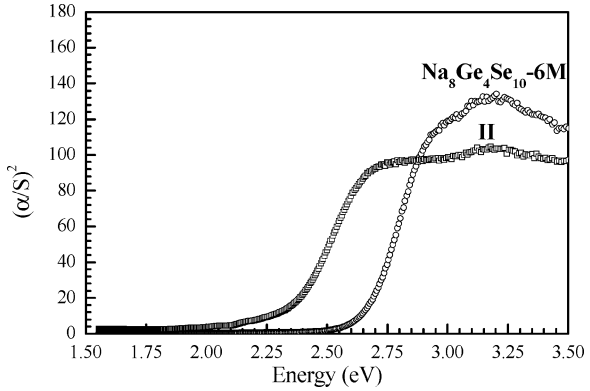

Figure 10. Diffuse reflectance spectra of $Na_8Ge_4Se_{10}$-6M and $Ag_xNa_{(8-x)}Ge_4Se_{10}$ ($x = 0.67$), **II**.

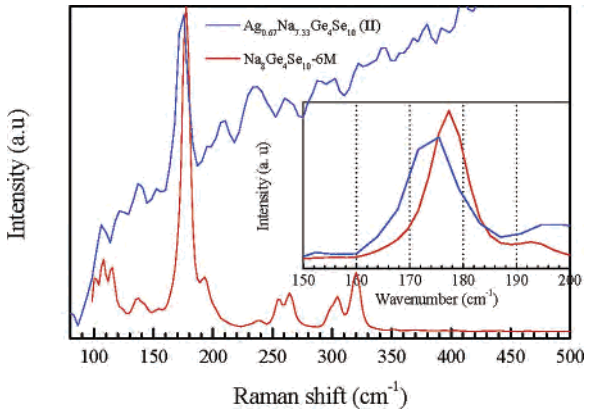

Figure 11. The Raman spectra of $Na_8Ge_4Se_{10}$-6M and $Ag_xNa_{(8-x)}Ge_4Se_{10}$ ($x = 0.67$), **II**.

because they lie far above the Fermi energy and are essentially ionic interactions with the Ge−Se network. But when Ag^+ ions substitute for Na^+, there is hybridization of Se with Ag and Ge orbitals, which may contribute to the top of valence band, thus a red-shift is observed. The narrowing of the band gap could be caused by the Ag−Ag ($d^{10}\cdots d^{10}$) interaction, which could create states below the conduction band. However, long Ag−Ag contacts (>4 Å) in these compounds (**I**−**VI**) preclude the possibility of any direct overlap of orbitals, thus minimizing its contribution (if any) toward decreasing the band gap. Theoretical band-structure calculations are required to explain clearly how the Ag orbitals contribute in the valence and conduction band in lowering the band gap.

Raman spectra for pure $Na_8Ge_4Se_{10}$-6M and one of the Ag^+-substituted compositions $Ag_{0.67}Na_{7.33}Ge_4Se_{10}$ (**II**) are shown in Figure 11. The Raman spectrum for the pure $Na_8Ge_4Se_{10}$-6M contains one strong peak centered at 177 cm^{-1} and several less-intense low-energy (137, 116, 107, and 100 cm^{-1}) and high-energy (255, 265, 304, and 321 cm^{-1}) peaks and is remarkably similar to the Raman spectrum of $Na_9Sm(Ge_2Se_6)_2$.[15b] The structure of $Na_9Sm(Ge_2Se_6)_2$ contains ethane-like $Ge_2Se_6^{6-}$ units, while "head to head−tail to tail" condensation of two ethane-like $Ge_2Se_6^{6-}$ units results in a chairlike 6-membered $Ge_4Se_{10}^{8-}$ unit found in $Na_8Ge_4Se_{10}$-6M.[2] So drawing upon a similar argument, we tentatively assign the peak at 177 cm^{-1} to a pseudosymmetric A1-type stretching vibration of $Ge_4Se_{10}^{8-}$ unit. The Raman spectrum of the Ag-substituted sample (**II**) is not well-resolved because of a broad luminescent background and the light sensitivity of the samples; however, one peak at 173 cm^{-1} can be observed consistently, which can be readily identified as the pseudosymmetric A1-type Ge−Se stretching vibration. Some differences can be observed between the pure and Ag-substituted sample. The band at 177 cm^{-1} in the spectrum of $x = 0$ is shifted down to 173 cm^{-1} for the sample with $x = 0.67$ (**II**) and is also slightly broadened asymmetrically (see inset of Figure 11). The red shift can be attributed to the net effect on Ge−Se force constant resulting from Ag substitution, which weakens the Ge−Se bonds through Ag−Se covalent overlap. The weakening of the Ge−Se bonds is reflected by their average Ge−Se bond lengths: 2.350(3) and 2.362(2) Å for $x = 0$ and $x = 0.67$ (**II**), respectively. The slight asymmetric broadening can be attributed to the disorder of Na and Ag position in the solid solution. Such phenomenon has been previously observed in the $BaSO_4$−$PbSO_4$ solid solutions.[30]

Conclusions

A new family of silver-substituted solids has been prepared by solid-state reactions. The successful incorporation of building-blocks in these compounds suggests that it is possible to design solids by replacing Na^+ with other metal ions from ternary Na−Ge−Q phases containing a building-block of one's choice. The proper reaction conditions using the alkali-chalcogenide flux or solid-state metathesis are required to maintain the structural integrity of the building-block. The analyses of the crystal structures reveal that Ag^+ ions prefer distorted Na^+ sites, which is important for predicting the site of Ag^+ substitution and for tailoring the properties. The preliminary optical property investigation indicates that the band gap can be fine-tuned by the amount of silver substitution.

Acknowledgment. The authors wish to acknowledge financial support provided by the National Science Foundation, NSF-DMR-0343412. A.L.K. received funding from the NSF-REU for Solid-State Chemistry.

Supporting Information Available: X-ray crystallographic data in CIF format for **I**−**VII** and a Table (S1) containing the selected geometrical parameters for **I**−**VII**. This material is available free of charge via the Internet at http://pubs.acs.org.

IC061064Z

(30) Lee, J.-S.; Wang, H.-R.; Lizuka, Y.; Yu, S.-C. Z. *Kristallogr*. **2005**, *220*, 1.